

Polar Biol (2013) 36:1483–1497
DOI 10.1007/s00300-013-1368-7

ORIGINAL PAPER

Effect of melting Antarctic sea ice on the fate of microbial communities studied in microcosms

D. Lannuzel · V. Schoemann · I. Dumont ·
M. Content · J. de Jong · J.-L. Tison ·
B. Delille · S. Becquevort

Received: 19 December 2012 / Revised: 13 June 2013 / Accepted: 28 June 2013 / Published online: 12 July 2013
© The Author(s) 2013. This article is published with open access at Springerlink.com

Abstract Although algal growth in the iron-deficient Southern Ocean surface waters is generally low, there is considerable evidence that winter sea ice contains high amounts of iron and organic matter leading to ice-edge blooms during austral spring. We used field observations and ship-based microcosm experiments to study the effect of the seeding by sea ice microorganisms, and the fertilization by organic matter and iron on the planktonic community at the onset of spring/summer in the Weddell Sea. Pack ice was a major source of autotrophs resulting in a ninefold to 27-fold increase in the sea ice-fertilized seawater microcosm compared to the ice-free seawater microcosm. However, heterotrophs were released in lower numbers (only a 2- to 6-fold increase). Pack ice was also an important source of dissolved organic matter for the planktonic community. Small algae (<10 µm) and bacteria released from melting sea ice were able to thrive in seawater. Field observations show that the supply

of iron from melting sea ice had occurred well before our arrival onsite, and the supply of iron to the microcosms was therefore low. We finally ran a “sequential melting” experiment to monitor the release of ice constituents in seawater. Brine drainage occurred first and was associated with the release of dissolved elements (salts, dissolved organic carbon and dissolved iron). Particulate organic carbon and particulate iron were released with low-salinity waters at a later stage.

Keywords Sea ice · Microbial community · Antarctica · Iron

Introduction

It is now well established that iron (Fe) supply and availability is of critical importance for phytoplankton growth in

D. Lannuzel (✉)
Institute for Marine and Antarctic Studies,
University of Tasmania, Locked Bag 129,
Hobart, TAS 7001, Australia
e-mail: delphine.lannuzel@utas.edu.au

D. Lannuzel
Antarctic Climate and Ecosystems CRC,
University of Tasmania, Private Bag 80,
Hobart, TAS 7001, Australia

D. Lannuzel
Laboratoire d’Océanographie Chimique et Géochimie des Eaux,
Université Libre de Bruxelles, Campus de la Plaine CP208,
Bd. du Triomphe, 1050 Bruxelles, Belgium

V. Schoemann · S. Becquevort
Ecologie des Systèmes Aquatiques, Faculté des Sciences,
Université Libre de Bruxelles, Campus de la Plaine CP 221,
Bd. du Triomphe, 1050 Bruxelles, Belgium

V. Schoemann · J. de Jong · J.-L. Tison
Laboratoire de Glaciologie (GLACIOL), Département des
Sciences de la Terre et de l’Environnement (DSTE), Faculté des
Sciences, Université Libre de Bruxelles, CP 160/03,
50 Av. F. D. Roosevelt, 1050 Brussels, Belgium

I. Dumont · M. Content · J. de Jong
Unité Isotopes Pétrologie et Environnement (IPE), Département
des Sciences de la Terre et de l’Environnement (DSTE), Faculté
des Sciences, Université Libre de Bruxelles, CP 160/02,
Avenue F.D. Roosevelt 50, 1050 Brussels, Belgium

B. Delille
Unité d’Océanographie Chimique, MARE, Université de Liège,
Allée du 6 Août, 17, 4000 Liège, Belgium

the high nutrient low chlorophyll (HNLC) Southern Ocean, where macro-nutrients levels are high but primary productivity remains low throughout the year due to widespread Fe limitation (Martin et al. 1990). There is evidence that sea ice is enriched in Fe and triggers ice-edge blooms when it melts in spring (Sedwick and DiTullio 1997; Lannuzel et al. 2010). Besides its role in storing Fe, sea ice can incorporate microorganisms (e.g. Gradinger and Ikävalko 1998; Rozanska et al. 2008), as well as organic matter (Thomas and Papadimitriou 2003; Becquevort et al. 2009) when it forms. Organisms trapped in sea ice can survive the extremely harsh winter conditions (restricted space to grow, low temperature and high salinity). When environmental conditions become favourable (light, temperature, salinity and nutrients), a large biomass of microorganisms then develop within the ice. When sea ice melts, these microorganisms, as well as organic and inorganic material (DOM and Fe), are released into a shallow and vertically stabilized water layer. This seasonal phenomenon produces ice-edge phytoplankton blooms visible on satellite pictures (Smith and Nelson 1986; Lancelot et al. 1993; Lancelot et al. 2009). The magnitude and duration of these blooms may vary widely in space and time (Arrigo et al. 2010 and references therein).

A small body of papers report laboratory experiments set-up to understand the mechanisms controlling ice-edge plankton blooms (Mathot et al. 1991; Riebesell et al. 1991; Kuosa et al. 1992; Giesenhagen et al. 1999). These experiments mainly focussed on the Atlantic sector of the Southern Ocean and the Weddell Sea. In each of these studies, the experimental protocols were tailored to address specific questions; Mathot et al. (1991) simulated the seeding of sea ice algae in filtered seawater and provided information on the potential photosynthetic activity and growth of the sea ice algae released in a planktonic environment. Riebesell et al. (1991) assessed the aggregation potential of ice algae using rolling tanks. Kuosa et al. (1992) performed aquarium experiments involving addition of unfiltered brown ice/slush into seawater to study the impact of sea ice microorganisms on the pelagic system. Similarly, Giesenhagen et al. (1999) ran microcosm experiments to separate the effects of the supply of organic matter from the effects of the supply of microorganisms on the microbial community and further investigated the loss of organic matter by sedimentation and/or grazing by copepods. However, none of these studies were conducted under trace-metal clean conditions, which limits our understanding of the role of Fe in the sea ice realm. In addition, none of the above mentioned studies investigated the sequence with which the nutritive elements (organic matter and Fe) and the microorganisms are released into seawater when sea ice melts.

This paper presents results from field observations during a time series and laboratory-based experiments

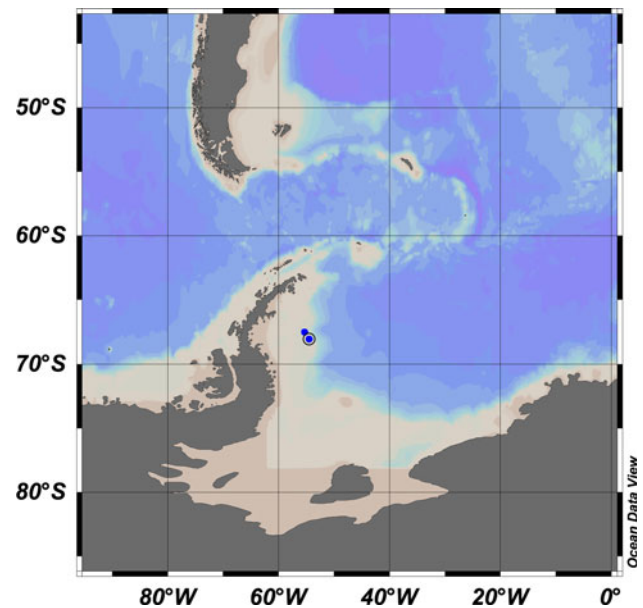


Fig. 1 Map of the sampling area (Schlitzer 2008). The blue dots mark the initial and final location of the ice floe

performed under trace-metal clean conditions, using sea ice and seawater collected during the 2004/2005 Ice Station POLarstern (ISPOL) research cruise in the Western Weddell Sea, Antarctica. First, an overview of the seasonal distribution of microorganisms, organic matter and Fe in 1st year pack ice is given. Then, results from microcosm experiments performed onboard to investigate the effect of microorganisms, organic matter and Fe released from sea ice on microbial communities at two different times of the spring-summer season are presented. A final and complementary experiment was conducted in the home laboratory to study the sequence of release of each of these constituents from melting sea ice into seawater.

Materials and methods

Field sampling

Samples were collected in the pack ice zone during the ISPOL research cruise onboard the RV *Polarstern* in the Western Weddell Sea, Antarctic Peninsula (68°S/55°W, Fig. 1) in November–December 2004. The RV *Polarstern* was anchored to a large ice floe (few km in size) in order to follow the temporal evolution of the physical, chemical and biological atmospheric–ice–ocean processes during the transition from austral spring to summer (Hellmer et al. 2008). Sampling of 1st year sea ice was conducted on a 20 m × 20 m site, located 1 km away from the research vessel, using precautions to avoid metal and organic matter contamination. Field operators worked upwind, wore clean

room garments (Tyvek overall, overshoes and polyethylene gloves) and used non-contaminating equipment to collect sea ice and seawater samples (Lannuzel et al. 2006; Dumont et al. 2009). Detail on the sampling site is reported in Tison et al. (2008).

The 90-cm-long ice cores were sliced into 6-cm-thick sections, transferred into acid-washed polyethylene containers and processed onboard for the analysis of Chlorophyll *a* (Chl*a*) and microscopic investigations. Sea ice sections were transferred into pre-combusted (450 °C, 4 h) glass beakers for dissolved organic carbon (DOC) and particulate organic carbon (POC) determination. Seawater (ice-water interface and 30 m depth) was collected using a portable peristaltic pump (Cole-Parmer, Masterflex E/P) and acid-cleaned C-flex tubing. Seawater samples were transferred into acid-washed bottles thoroughly rinsed with the collected samples. Sampling was carried out on seven occasions, between 29 November 2004 and 30 December 2004, at regular time intervals (typically every 5 days) to study the vertical and seasonal distribution of the microbial communities in the sea ice environment.

Measured parameters

Temperature, salinity and brine volume fraction

Sea ice texture, temperature and salinity of the ice cover were determined as detailed in Tison et al. (2008). Brine volume fraction was calculated from temperature and salinity data following Cox and Weeks (1998) and Eicken (2003). During the sequential melting experiment in the home laboratory, seawater temperature was monitored using a general-purpose laboratory thermometer, and the salinity was determined using a portable salinometer Global Water PC300 with an accuracy of ± 0.003 .

Iron

Sea ice sections were melted in the dark at 4 °C and then passed through 0.2- μm polycarbonate filters. Seawater samples and microcosm sub-samples were filtered the same way. Plasticware (low density polyethylene LDPE and high density polyethylene HDPE) used for trace-metal work was cleaned as follows: first soaked in a detergent bath (RBS 5 % v:v) for 24 h, followed by three rinses with deionized water and three rinses with ultra high purity water (UHP) (18.2 M Ω Millipore milli-Q system) before being filled with 6 M HCl (Merck, reagent grade) for 1 week. In a trace-metal clean room, items were then rinsed five times with UHP water and dried inside a class-100 laminar flow hood. Twenty litre polycarbonate (PC) carboys (Nalgene) used for microcosms were treated the same way, albeit a weaker acid soak (1 M HCl, Merck, reagent grade).

Acid-cleaned bottles and containers were sealed in triple plastic bags until use. PC filters (0.2 μm porosity, 47 mm diameter, Nuclepore) were treated in 1 M HCl ultrapure (Ultrex, JT Baker) for 1 week before being gently rinsed five times and stored in UHP until use. Samples collected for Fe analysis were stored in acid-cleaned LDPE bottles and acidified to pH 1.8 with ultrapure HNO₃ (Ultrex, JT Baker). Total dissolvable Fe (TDFe, unfiltered) and dissolved Fe (DFe, filtered through 0.2- μm Nuclepore PC filters) samples from the microcosms were measured onboard by flow injection analysis following Lannuzel et al. (2006). TDFe samples from the sequential experiment were analysed in the home laboratory 6 months after collection by isotopic dilution combined with multiple collector inductively coupled plasma mass spectrometry (IDMC-ICP-MS) using nitrilotriacetic acid chelating resin for pre-concentration and matrix separation (de Jong et al. 2008).

Dissolved and particulate organic carbon

POC was collected on pre-combusted (450 °C, 4 h) Whatman GF/F filters and stored in polystyrene petri dishes at -20 °C until analysis. After drying the filters at 60 °C, inorganic carbon was removed by adding 100 μL of concentrated Hydrochloric acid (HCl, Merck Suprapure) on the filters. POC then was analysed with a Fisons NA-1500 elemental analyser. Filtered samples for DOC were stored in pre-combusted (450 °C, 4 h) 20-ml glass ampoules with 25 μL H₃PO₄ (Merck, Suprapure) and sealed to avoid contact with the atmosphere. Samples were kept in the dark at 4 °C until analysis. DOC was measured by high temperature catalytic oxidation (HTCO; procedure of Sugimura and Suzuki 1988) with a Dohrmann Apollo 9000 instrument.

Chlorophyll a

Ice core sections were melted in the dark at 4 °C in 0.2- μm -prefiltered seawater (1:4, v:v) and filtered onto 0.8- μm GF/F filters (Whatmann) for the determination of Chl*a*. Sub-samples from the microcosm experiments were sequentially filtered onto 10- and 0.8- μm GF/F filters (Whatmann). Pigments deposited on the filters were then extracted in 90 % (v:v) acetone in the dark at 4 °C for 24 h and quantified using a Kontron SFM 25 fluorometer calibrated with a Chl*a* standard solution (*Anacystis nidulans* algae, Sigma) according to Yentsch and Menzel (1963).

Abundance and biomass of bacteria, algae and protozoa

Ice core sections sampled for the determination of abundance and biomass of microorganisms were melted in the dark at 4 °C in 0.2- μm -prefiltered seawater (1:4, v:v).

Algae and protozoa from the melted ice, seawater and microcosms were enumerated by inverted light microscopy (Utermöhl 1958) and by epifluorescence microscopy after DAPI staining (Porter and Feig 1980) as explained in details in Becquevort et al. (2009). Algae and protozoa biomasses were estimated from cell biovolumes using a set of geometric correspondences (Hillebrand et al. 1999) and specific carbon to volume relationship (Menden-Deuer and Lessard 2000). In the microcosms experiments, protozoa biomass was assessed on the 1st and last day of the experiment. Bacteria were enumerated by epifluorescence after DAPI staining. A minimum of 100 cells were counted in at least 20 different fields at 1,000 times magnification. Bacterial biovolumes were determined by image analysis (Lucia 4.6 software) using geometric (Watson et al. 1977) and converted to carbon biomass using carbon to volume relationships (Simon and Azam 1989): $C = 92 V^{0.598}$ where C is the carbon per cell (fg C cell^{-1}) and V is the biovolume (μm^3).

Experiments

Microcosms

The four microcosms were set up following Mathot et al. (1991) and Giesenhausen et al. (1999) protocols. Our priority being the prevention of contamination, handling of the samples was carried out in a clean container under a Class-100 trace-metal clean laminar flow hood. The experiment was conducted on 09 December (A) and on 25 December (B) using sea ice (bottom section) and seawater (30 m deep). Seawater was pre-filtered using 0.2- μm membrane cartridges (Sartobran 300 sterile capsule). A 10-cm section of bottom sea ice was thawed in 3 L of filtered seawater (1:4, v:v) at 4 °C in the dark (total volume sea ice + seawater = 3.7 L). One litre of this solution was then filtered (SI_f) onto 0.2- μm acid-cleaned PC filter (Nuclepore), using a PC Sartorius filtration unit and a hand-pump (Nalgene).

The first 20-L PC carboy contained only unfiltered seawater (SW_{unf}) and was used as a control to follow the growth of the planktonic community in ice-free waters. The second microcosm ($\text{SW}_{\text{unf}} + \text{SI}_{\text{unf}}$) was a mix of 20 L of unfiltered seawater and 1 L of the sea ice solution and was meant to mimic natural conditions. The third microcosm ($\text{SW}_f + \text{SI}_{\text{unf}}$) aimed at studying the fate of sea ice organisms in seawater. In this case, 1 L of sea ice solution was added to 20 L of filtered seawater. Finally, the fourth microcosm ($\text{SW}_{\text{unf}} + \text{SI}_f$) was 20 L of seawater spiked with 1 L of filtered sea ice solution. $\text{SW}_{\text{unf}} + \text{SI}_f$ was meant to assess the growth of planktonic organisms when sea ice melts (Table 1). The final sea ice to seawater

volume ratio was 1:80, which represents the melting of 10-cm-thick sea ice in an 8 m deep mixed layer.

The 20-L carboys were incubated at -1 °C in the ship's culture room and exposed to a continuous light intensity of $45 \mu\text{E m}^{-2} \text{s}^{-1}$. The carboys were sub-sampled under trace-metal clean conditions almost daily for 10 days in order to follow the evolution of DOC, POC and microorganisms (algae, bacteria and protozoa). Protozoan biomass was assessed on the 1st and last days of the microcosm experiments. Total dissolvable Fe (TDFe, unfiltered, pH 1.8) was measured at the start of the two experiments. DFe represents the fraction of Fe readily available for biological uptake, while TDFe represents the fraction of Fe that can become bioavailable for microorganisms (e.g. via remineralization processes). We therefore chose to consider TDFe rather than DFe.

Sequential melting

A final experiment was performed in the home laboratory under temperature controlled and trace-metal clean conditions to study the release of sea ice components (salt, organic matter and Fe). Equipment in contact with the seawater and/or sea ice was acid-cleaned before the start of the experiment. Seawater used in this experiment was collected during the CLIVAR SR3 cruise in the Antarctic Pacific sector (135–150°E) in December 2001. A volume of 13.57 L was filtered through a 0.2- μm Sartobran® 300 cartridge and transferred in a 20-L HDPE container, at 2 °C, in the dark. The melting chamber simulated the melting of sea ice as the air temperature increased, without increasing the seawater temperature. Constant mixing was applied, and a tube filled with ethanol connected to a thermostatic water bath helped maintain seawater at -1.9 °C. A 20-cm-thick frozen bottom ice section (diameter = 14 cm; melted volume = 1.54 L) sampled on 04 December during ISPOL was allowed to melt into this 20-L HDPE container filled with seawater (final sea ice to seawater volume ratio $\approx 1:10$). Meltwater was sampled using a peristaltic pump (Masterflex) and a tube placed at the bottom of the HDPE container. Salinity, temperature, TDFe, DOC and POC concentrations were monitored until complete melting of the ice was achieved (54 h). For each sampling at time (t), a second meltwater sample (t') was collected and left in the chamber until the time step ($t + 1$). This was done to obtain the contribution of sea ice melting only ($C_{t+1} - C_t$). For each parameter, fluxes from the sea ice were estimated using the equation $F_{t+1} = (C_{t+1} - C_t) \cdot V/t$, with C the concentration of the compound, V the volume of solution left in the carboy and t the time elapsed between $t + 1$ and t . V takes into account the volume of melted sea ice added (averaged melting rate = 28.2 mL h^{-1}) as well as the volume of solution sub-sampled at each time step.

Table 1 Characteristics of the microcosms experiments A and B

Microcosm	Seawater	Sea ice	Aim of the microcosm
SW _{unf}	Unfiltered	None	Growth of planktonic biota without sea ice
SW _{unf} + SI _{unf}	Unfiltered	Unfiltered	“Natural” simulation
SW _f + SI _{unf}	Filtered	Unfiltered	Growth of ice-derived biota in seawater
SW _{unf} + SI _f	Unfiltered	Filtered	Impact of ice-derived nutrients on planktonic biota

Results

Field observations

Sea ice thermodynamics

Detailed thermodynamics and chemical properties of the ISPOL drifting station are presented in Tison et al. (2008) and Lannuzel et al. (2008). To summarize, the visited ice floe was approximately 90-cm-thick 1st year sea ice with a 10-cm layer of granular ice (frazil) underlain with columnar ice (Tison et al. 2008). The freeboard was positive during the whole time series. Ice temperatures in the visited area were above -5°C and showed clear signs of warm “spring–summer” regime (Table 2). Brine volume fractions indicate that the ice cover was highly permeable upon arrival on site, with values greater than the 5 % permeability threshold along the entire profile (Golden et al. 1998; Table 2). The beginning of the sampling period was characterized by intense gravity-driven brine drainage. As brine salinity became lower than seawater salinity, molecular diffusion, a much slower process, then took place as the principal pathway for the transfer of dissolved material at the ice-water interface.

Iron, organic matter and Chla

TDFe concentrations ranged from 2.3 to 97.8 nmol L⁻¹ in sea ice and from 0.5 to 4.1 nmol L⁻¹ in underlying seawater (Table 2). DOC and POC concentrations in sea ice ranged, respectively, from 1,273 to 8,413 $\mu\text{g C L}^{-1}$ and from 93 to 5,640 $\mu\text{g C L}^{-1}$. Maximum POC values were measured in the bottom layers, while lower values were observed in intermediate layers. In seawater, POC ranged between 12 and 130 $\mu\text{g C L}^{-1}$, while DOC was unfortunately not measured. Chla ranged from 0.08 to 28.41 $\mu\text{g L}^{-1}$ in sea ice with the maximum values observed in basal ice. Seawater Chla increased with time (0.03 to 0.21 $\mu\text{g L}^{-1}$) and remained always lower than in sea ice.

Autotrophs

Taxonomic similarity between the ice-derived and planktonic communities was observed during the time series

(Fig. 2). Autotrophic microorganisms represented $82 \pm 16\%$ of the total biomass in sea ice, especially in the surface ($90 \pm 7\%$) and bottom ice layers ($96 \pm 7\%$). In surface sea ice (3–9 cm), *Phaeocystis* single cells dominated in terms of abundance and biomass. Some colonies were also observed, but their biomass remained low. In contrast, pennate diatoms dominated the abundance and the biomass of the autotrophic microorganisms in the bottom sea ice. *Fragilariopsis* sp. was the main pennate diatom present in abundance and biomass in surface sea ice. In bottom sea ice, *Cylindrotheca* sp. and *Nitzschia* (<10 μm) were the most abundant, whereas in term of biomass, *Amphiprora* sp. (>10 μm) became predominant.

In seawater, autotrophic organisms represented $41 \pm 13\%$ of the total biomass. *Phaeocystis* single cells were the most abundant. However, the pattern of species in seawater was patchier than in sea ice (Fig. 2), with for example autotrophic dinoflagellates contributing to $9 \pm 7\%$ of the total biomass. A more heterogeneous distribution of pennate diatoms (*Fragilariopsis* sp.) and centric diatoms (*Chaetoceros* sp., *Biddulphia* sp., *Corethron* sp.) was also observed. At 30 m deep, autotrophic biomasses increased fivefold between the 29 November and the 30 December, due to an increase in pennate and centric diatoms.

Heterotrophs

Heterotrophic microorganisms (bacteria and protozoa) were present in the ice, with protozoa accounting for $48 \pm 23\%$ of the total heterotrophic biomass. The distribution of protozoa showed maximum concentrations in the bottom ice (Fig. 2). The protozoan biomass was mainly composed of flagellates, dinoflagellates and sarcodines. The protozoan biomass showed exceptionally high value on the 30 December in bottom ice (507.51 $\mu\text{g C L}^{-1}$). The bacterial biomass ranged from 1.75 to 13.83 $\mu\text{g C L}^{-1}$ in sea ice, with a fairly homogeneous distribution along the ice core.

In seawater, protozoa biomass varied between 0.12 and 2.90 $\mu\text{g C L}^{-1}$ and was mainly composed of flagellates, dinoflagellates and ciliates (Fig. 2). The protozoan biomass increased over time and reached maximum concentration on 19 December in surface waters and then decreased.

Table 2 Summary of sea ice temperature (Temp), brine volume fraction (Vb/V), Chlorophyll *a* (Chl*a*), particulate organic carbon (POC), dissolved organic carbon (DOC) and total dissolvable iron (TDFe) concentrations in sea ice and seawater during the ISPOL time series

Date dd-mm-yyyy	Type of sample	Depth	Temp °C	Vb/V %	Chl <i>a</i> µg L ⁻¹	TDFe nmol L ⁻¹	POC µg L ⁻¹	DOC µg L ⁻¹
29-Nov-2004	Sea ice	3–9 cm	−3.1	15	0.36	57	684	<i>na</i>
	Sea ice	9–15 cm	−2.4	16	0.41	57	541	<i>na</i>
	Sea ice	40–46 cm	−2.3	13	0.18	21.7	172	<i>na</i>
	Sea ice	60–66 cm	−2.1	11	0.08	42.6	112	<i>na</i>
	Sea ice	78–84 cm	−2	14	3.98	<i>na</i>	621	<i>na</i>
	Sea ice	84–90 cm	−1.9	26	23.57	97.8	3,766	<i>na</i>
	Seawater	0 m			0.030	1.4	33	<i>na</i>
	Seawater	1 m			0.038	1.5	< <i>dl</i>	<i>na</i>
	Seawater	30 m			0.033	1.6	1	<i>na</i>
4-Dec-2004	Sea ice	3–9 cm	−1.7	16	0.44	55.1	565	<i>na</i>
	Sea ice	9–15 cm	−2.1	13	0.44	<i>na</i>	428	<i>na</i>
	Sea ice	40–46 cm	−1.9	13	0.45	10.1	167	8,004
	Sea ice	60–66 cm	−1.6	8	0.16	8.2	232	4,662
	Sea ice	78–84 cm	−1.8	14	3.44	<i>na</i>	741	4,109
	Sea ice	84–90 cm	−1.8	25	26.47	21.2	3,175	8,413
	Seawater	0 m			0.05	1.6	< <i>dl</i>	<i>na</i>
	Seawater	1 m			0.05	1.7	3	<i>na</i>
	Seawater	30 m			0.05	<i>na</i>	<i>na</i>	<i>na</i>
9-Dec-2004	Sea ice	3–9 cm	−1.2	15	0.97	22.7	595	2,452
	Sea ice	9–15 cm	−1.4	16	2.22	<i>na</i>	903	5,669
	Sea ice	40–46 cm	−1.9	14	0.4	2.7	279	3,104
	Sea ice	60–66 cm	−1.8	14	0.25	5.1	191	5,212
	Sea ice	78–84 cm	−1.8	17	2.56	<i>na</i>	1,138	1,656
	Sea ice	84–90 cm	−1.8	14	21.48	12.5	4,754	5,649
	Seawater	0 m			0.06	2.6	24	<i>na</i>
	Seawater	1 m			0.06	1.6	< <i>dl</i>	<i>na</i>
	Seawater	30 m			0.06	<i>na</i>	13	<i>na</i>
14-Dec-2004	Sea ice	0–9 cm	−1.5	25	0.69	19.3	725	6,845
	Sea ice	9–15 cm	−1.4	17	1.23	7.1	766	4,152
	Sea ice	40–46 cm	−1.7	11	0.27	5.3	327	4,483
	Sea ice	60–66 cm	−1.7	10	0.3	3.5	451	3,856
	Sea ice	74–80 cm	−1.8	12	2.19	<i>na</i>	773	5,305
	Sea ice	80–86 cm	−1.9	21	24.23	22	5,640	5,717
	Seawater	0 m			0.06	1.8	56	<i>na</i>
	Seawater	1 m			0.1	0.5	58	<i>na</i>
	Seawater	30 m			0.09	1.8	36	<i>na</i>
19-Dec-2004	Sea ice	4–10 cm	−0.4	33	0.78	24.7	282	3,629
	Sea ice	10–16 cm	−1.3	30	1.06	<i>na</i>	306	3,561
	Sea ice	40–46 cm	−1.4	17	0.2	5.1	181	3,615
	Sea ice	60–66 cm	−1.5	11	0.65	3	223	2,408
	Sea ice	77–83 cm	−1.6	10	4.21	<i>na</i>	618	3,179
	Sea ice	83–89 m	−1.6	16	28.41	14.7	2,061	4,242
	Seawater	0 m			0.11	3.2	69	<i>na</i>
	Seawater	1 m			0.09	2.2	162	<i>na</i>
	Seawater	30 m			0.13	<i>na</i>	46	<i>na</i>

Table 2 continued

Date dd-mm-yyyy	Type of sample	Depth	Temp °C	Vb/V %	Chla $\mu\text{g L}^{-1}$	TDFe nmol L^{-1}	POC $\mu\text{g L}^{-1}$	DOC $\mu\text{g L}^{-1}$
25-Dec-2004	Sea ice	3–9 cm	−0.2	11	0.7	10.7	93	na
	Sea ice	9–15 cm	−0.7	14	0.66	na	242	na
	Sea ice	40–46 cm	−1.2	21	0.69	4	146	na
	Sea ice	60–66 cm	−1.2	16	0.29	2.3	148	na
	Sea ice	74–84 cm	−1.2	15	3.3	na	496	na
	Sea ice	84–90 cm	−1.4	17	16.33	8.4	2,515	na
	Seawater	0 m			0.21	2.4	38	na
	Seawater	1 m			0.16	1.6	<dl	na
	Seawater	30 m			0.12	2.3	94	na
30-Dec-2004	Sea ice	3–9 cm	−1.1	20	1.69	14.1	357	5,255
	Sea ice	9–16 cm	−1.2	16	0.97	na	342	5,488
	Sea ice	40–46 cm	−1.4	13	0.59	4.8	364	2,762
	Sea ice	59–65 cm	−1.4	9	0.95	2.7	na	1,273
	Sea ice	74–80 cm	−1.6	11	3.62	na	534	1,273
	Sea ice	80–86 cm	−1.8	17	24.77	15.8	2,008	2,494
	Seawater	0 m			0.14	2.3	64	na
	Seawater	1 m			0.14	1.5	124	na
	Seawater	30 m			0.15	4.1	41	na

DOC and POC are reported in Dumont et al. (2009). Iron data are presented in Lannuzel et al. (2008)

na not assessed, < dl below detection limit

The bacterial biomass in seawater ranged from 0.37 to 1.71 $\mu\text{g C L}^{-1}$. Like protozoa, values were maximal on 19 December, but no clear seasonal trend was observed over the sampling period.

Microcosms

Supply of microorganisms, organic carbon and iron into the water column

When comparing $\text{SW}_{\text{unf-A}}$ and $\text{SW}_{\text{unf-B}}$ with SW_{unf} + $\text{SI}_{\text{unf-A}}$ and SW_{unf} + $\text{SI}_{\text{unf-B}}$, we can estimate the supply of autotrophs, heterotrophs, Fe, DOC and POC from melting sea ice into seawater (Table 3). Total biomasses (algae, bacteria and protozoa) were lower at the start of $\text{SW}_{\text{unf-A}}$ than $\text{SW}_{\text{unf-B}}$, suggesting a growth of microorganisms between the two sampling dates. This result is in agreement with our field observations in deep seawater between 9 December and 25 December (Fig. 2). However, we note that the microcosm SW_{unf} exhibits lower initial biomasses of phytoplankton and bacteria than the in situ sample in both experiments. The discrepancies between laboratory and field samples may be due to the grazing by protozoa during the 2 days (= melting time) elapsed between the sampling and the start of the microcosm experiments.

At the start of experiments $\text{SW}_{\text{unf-A}}$ and $\text{SW}_{\text{unf-B}}$ (9-Dec and 25-Dec), the autotrophic abundance was dominated by nanoflagellates, followed by dinoflagellates and ciliates. The autotrophic biomass was equally distributed between diatoms, nano- and dinoflagellates. The diatom biomass was mainly composed of pennates (*Fragilariopsis* sp.), even though some centrics were present in $\text{SW}_{\text{unf-A}}$ and even more centric was observed in $\text{SW}_{\text{unf-B}}$ (*Chaetoceros* sp.). Diatoms then became the dominant group both in terms of abundance and biomass when sea ice was added (SW_{unf} + SI_{unf}) in A (dominated by *Amphiprora* sp.) and B (dominated by *Cylindrotheca* sp.). The dino- and nanoflagellates biomass remained constant. The 1 % of sea ice added to seawater was therefore a major supply of algal biomass, especially pennate diatoms, in both experiments (9- to 27-fold increase; Table 3). Table 3 also indicates that sea ice supplied less heterotrophs (2- to 6-fold increase in the biomass of bacteria and protozoa) than autotrophs. The protozoan abundances were actually similar in $\text{SW}_{\text{unf-A}}$ and SW_{unf} + $\text{SI}_{\text{unf-A}}$, while the protozoan biomass only slightly increased in SW_{unf} + $\text{SI}_{\text{unf-A}}$ compared to $\text{SW}_{\text{unf-A}}$ (Table 3). In experiment B, we observed a slight increase in SW_{unf} + SI_{unf} compared to SW_{unf} both in terms of protozoan abundance (5 % increase) and biomass (20 % increase, Table 3). If bacterial abundance were similar in $\text{SW}_{\text{unf-B}}$ and SW_{unf} + $\text{SI}_{\text{unf-B}}$ at the start of the experiment, bacterial biomass was slightly higher in SW_{unf} + $\text{SI}_{\text{unf-B}}$ than

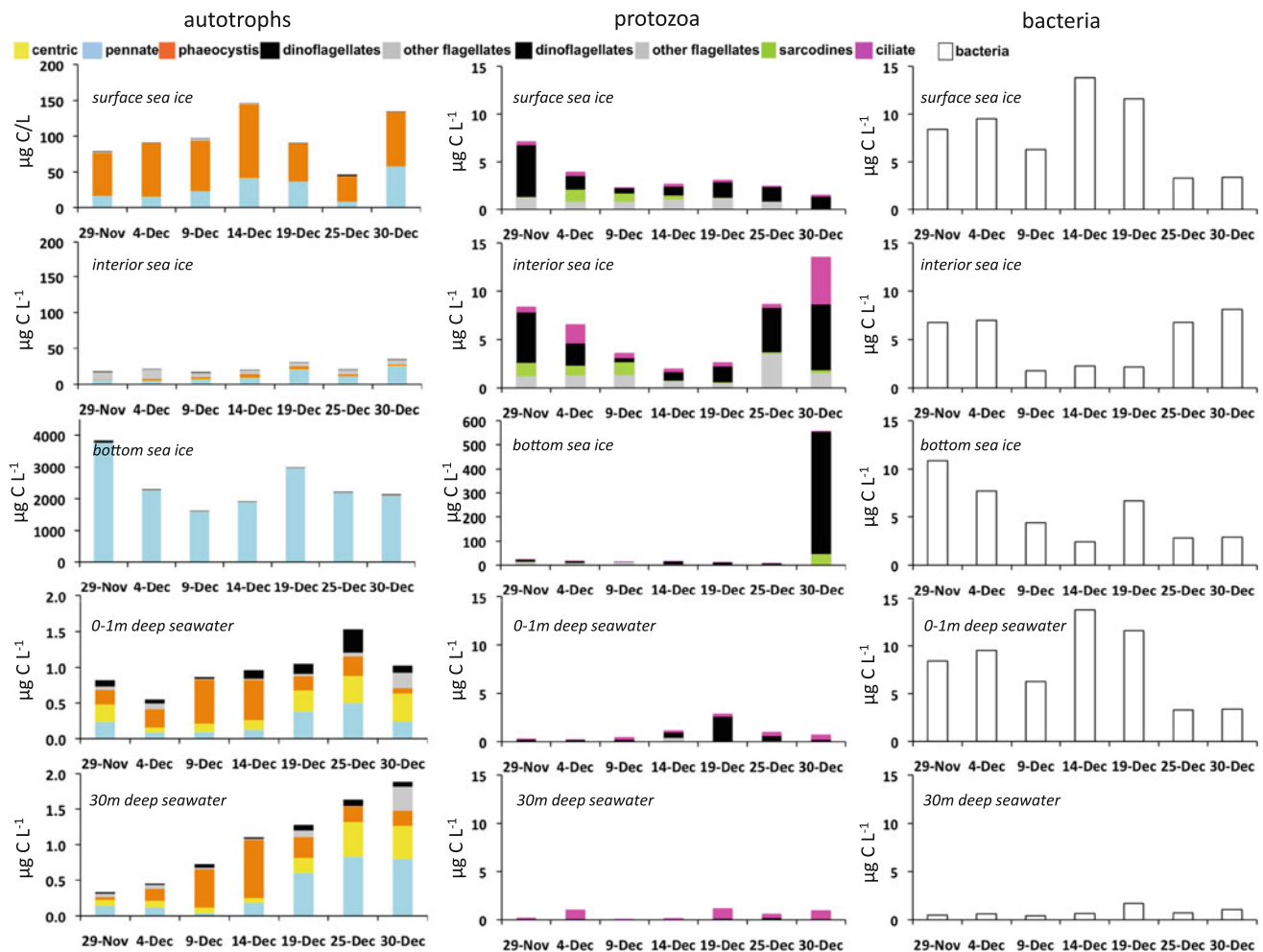


Fig. 2 Biomass distribution of autotrophs, protozoa and bacteria (in $\mu\text{g C L}^{-1}$) in sea ice and seawater during the ISPOL time series. Partial taxonomic similarity is observed between the ice-derived and planktonic communities during the time series

in $\text{SW}_{\text{unf-B}}$. In experiment A, bacterial abundance and biomass were surprisingly even lower in $\text{SW}_{\text{unf}} + \text{SI}_{\text{unf-A}}$ than in $\text{SW}_{\text{unf-A}}$. Consequently, the sea ice addition decreased the initial heterotroph to autotroph ratios from 2 for SW_{unf} to 0.05 for $\text{SW}_{\text{unf}} + \text{SI}_{\text{unf-A}}$ and 0.28 for $\text{SW}_{\text{unf}} + \text{SI}_{\text{unf-B}}$.

An important supply of DOC and POC was observed when sea ice was added to seawater (Table 3, DOC not

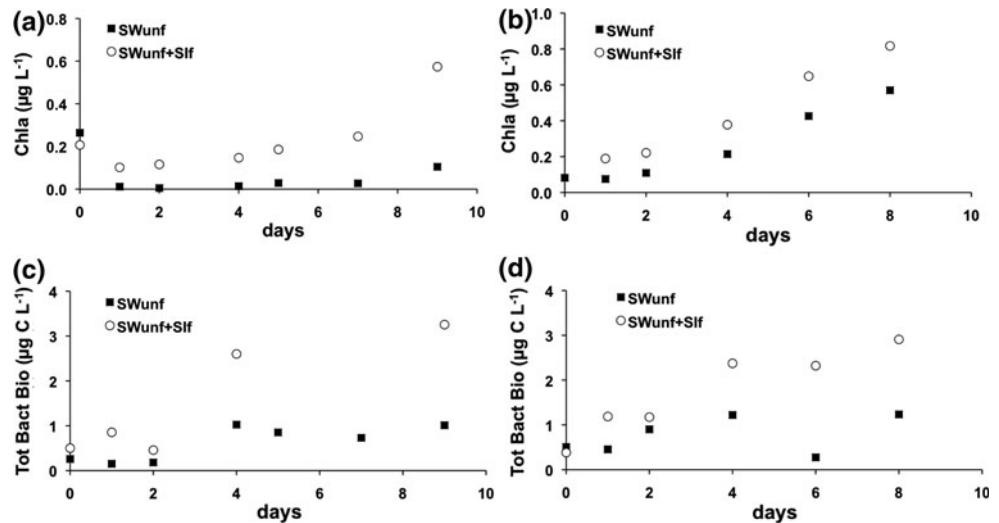
measured for A). Natural seawater samples also demonstrated an increase in organic matter concentration during sea ice melting (Table 2). This increase may be due to phytoplankton growth and not solely to the seeding of POC from sea ice. On the other hand, and based on the observed concentration in the field in 30 m deep seawater (2.3 nmol L^{-1}) and in bottom sea ice ($8.4\text{--}12.5 \text{ nmol L}^{-1}$), the addition of sea ice to seawater would have only

Table 3 Initial concentrations of microorganisms (algae, bacteria and protozoa), dissolved and particulate organic carbon (DOC and POC), and total dissolvable iron (TDFe) in microcosms SW_{unf} and $\text{SW}_{\text{unf}} + \text{SI}_{\text{unf}}$ for experiments A and B

		A		B	
		SW_{unf}	$\text{SW}_{\text{unf}} + \text{SI}_{\text{unf}}$	SW_{unf}	$\text{SW}_{\text{unf}} + \text{SI}_{\text{unf}}$
Algae	$\mu\text{g C L}^{-1}$	0.16	4.45	0.64	6.28
Bacteria	$\mu\text{g C L}^{-1}$	0.26	0.14	0.51	0.68
Protozoa	$\mu\text{g C L}^{-1}$	0.05	0.08	0.82	1.01
DOC	$\mu\text{g C L}^{-1}$	na	na	2,000	13,000
POC	$\mu\text{g C L}^{-1}$	167	318	95	127
TDFe	nmol L^{-1}	1.6	1.7	2.3	2.4

na not assessed

Fig. 3 **a** Chlorophyll *a* in the microcosms SW_{unf} and SW_{unf} + SI_f for experiments A, **b** Chlorophyll *a* in the microcosms SW_{unf} and SW_{unf} + SI_f for experiments B, **c** total bacterial biomass in the microcosms SW_{unf} and SW_{unf} + SI_f for experiments A and **d** total bacterial biomass in the microcosms SW_{unf} and SW_{unf} + SI_f for experiments B. Chl*a* associated with planktonic algae reached higher concentrations after 9 days in SW_{unf} + SI_f than SW_{unf}. Planktonic bacterial growth was similarly stimulated by the sea ice addition



contributed to an increase of 4–5 % of the initial seawater concentration of Fe in the microcosms. This estimate is confirmed by the slightly higher TDFe concentrations measured at the start in SW_{unf} + SI_{unf} compared to SW_{unf} (Table 3).

Supply of dissolved elements to the planktonic community

We showed here above that sea ice supplies microorganisms, organic carbon (dissolved and particulate) and Fe to a lesser extent in this study to seawater. The impact of sea ice in supplying key ingredients to seawater was further evaluated by comparing the growth of planktonic microorganisms in SW_{unf} and SW_{unf} + SI_f. For both assays, Chl*a* associated

with planktonic algae reached higher concentrations after 9 days in SW_{unf} + SI_f than in SW_{unf} (Fig. 3). Chl*a* increased from 0.20 to 0.57 μg L⁻¹ in SW_{unf} + SI_f-A and from 0.08 to 0.82 μg L⁻¹ in SW_{unf} + SI_f -B (Fig. 3). This indicates a stimulation of planktonic algal growth in response to the addition of dissolved nutrients supplied from sea ice. Note that Chl*a* increased in SW_{unf}-B (seawater only). This could result from the relatively high initial Fe concentration in seawater on 25 December (i.e. TDFe = 2.3 nmol L⁻¹) as well as favourable conditions inherent to bottle experiments (such as light and exclusion of mesozooplankton grazing).

Planktonic bacterial growth was similarly stimulated by the addition of filtered sea ice (Fig. 3). After respectively 9 and 8 days, total bacterial biomass increased sevenfold to eightfold in SW_{unf} + SI_f -A and SW_{unf} + SI_f -B, whereas it

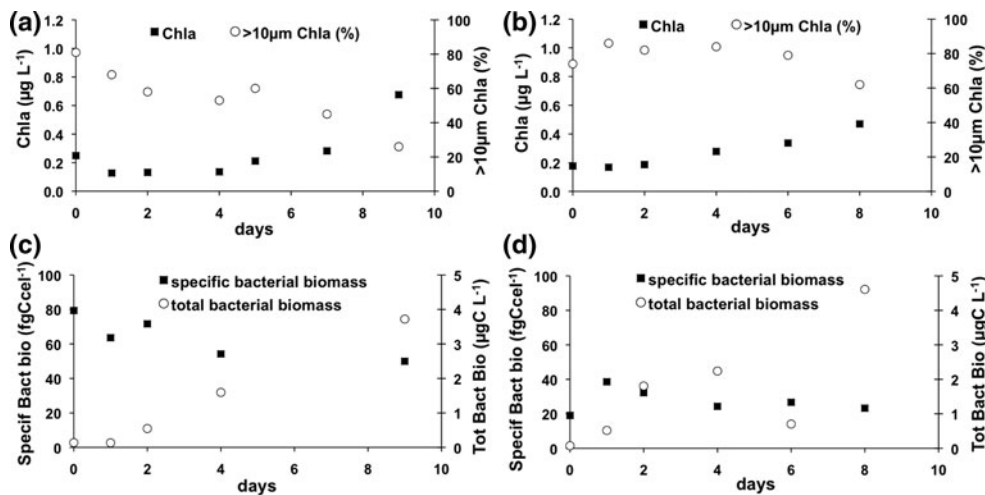


Fig. 4 **a** Chlorophyll *a* and percentage of Chlorophyll *a* > 10 μm in the microcosm SW_f + SI_{unf} for experiment A, **b** Chlorophyll *a* and percentage of Chlorophyll *a* > 10 μm in the microcosm SW_f + SI_{unf} for experiment B, **c** specific bacterial biomass (fg C cel⁻¹) and total bacterial biomass (μg C L⁻¹) in the microcosm SW_f + SI_{unf} for

experiment A and **d** specific bacterial biomass (fg C cel⁻¹) and total bacterial biomass (μg C L⁻¹) in the microcosm SW_f + SI_{unf} for experiment B. We observed the growth of the ice-derived algae and bacteria in filtered seawater

only increased two to fourfold in $SW_{\text{unf}}\text{-A}$ and $SW_{\text{unf}}\text{-B}$. Like *Chla* and bacteria, the protozoan biomass, particularly heterotrophic dinoflagellates, increased from 0.06 to 1.21 $\mu\text{g C L}^{-1}$ in $SW_{\text{unf}} + SI_{\text{f}}\text{-A}$ and from 0.79 to 3.62 $\mu\text{g C L}^{-1}$ in $SW_{\text{unf}} + SI_{\text{f}}\text{-B}$ (protozoa were only enumerated at the start and the end of the microcosms).

Evolution of ice-derived microorganisms in seawater

The microcosm $SW_{\text{f}} + SI_{\text{unf}}$ was designed to study the fate of sea ice microorganisms in seawater. After a latent period of 2 days, *Chla* increased from 0.25 to 0.68 $\mu\text{g L}^{-1}$ after 9 days in A (Fig. 4) and from 0.18 to 0.47 $\mu\text{g L}^{-1}$ after 8 days in B (Fig. 4). This shows that at least some of the ice-derived autotrophic organisms were able to grow in filtered seawater. Nevertheless, *Chla* associated with algae $>10 \mu\text{m}$ decreased with time, particularly in A (Fig. 4), indicating that algae $<10 \mu\text{m}$ were the ones growing. This result is in accordance with the shift in taxonomic composition of the algal assemblages from a dominance of *Amphiprora* sp. ($>10 \mu\text{m}$) at time zero to *Fragilariopsis* sp. ($<10 \mu\text{m}$) after 9 days. Similarly, sea ice bacteria seemed able to grow in seawater as shown by the increase in total biomass from 0.14 to 3.72 $\mu\text{g C L}^{-1}$ after 9 days in A and from 0.07 to 4.71 $\mu\text{g C L}^{-1}$ after 8 days in experiment B (Fig. 4). Like algae, a decrease in the size of bacteria was observed and specific carbon content decreased from 79 to 50 fg C cel^{-1} in A and from 53 to 24 fg C cel^{-1} in B (Fig. 4). While the protozoa biomass decreased from 2.92 to 0.82 $\mu\text{g C L}^{-1}$ in A, it did increase from 1.27 to 3.83 $\mu\text{g C L}^{-1}$ in B when the highest bacterial size attenuation was observed (protozoa were only enumerated at the start and the end of the microcosms).

Competition between ice-derived and planktonic microorganisms

The fore-mentioned microcosms (SW_{unf} , $SW_{\text{f}} + SI_{\text{unf}}$ and $SW_{\text{unf}} + SI_{\text{f}}$) intentionally exclude the direct interactions between ice-derived and planktonic microorganisms to study their effects independently. Nevertheless, competition between microorganisms, e.g. inorganic and organic nutrients, can occur in situ and result in a decrease of biomass. To study these natural interactions during sea ice melting (although grazing processes may be restricted in bottle studies), the distribution of the ice-derived and planktonic biomasses was studied together in $SW_{\text{unf}} + SI_{\text{unf}}$. By comparing the values obtained in $SW_{\text{unf}} + SI_{\text{unf}}$ to the sum of the values obtained in $SW_{\text{f}} + SI_{\text{unf}}$ and $SW_{\text{unf}} + SI_{\text{f}}$, we can estimate the magnitude of the interaction between ice-derived and planktonic microorganisms. *Chla* concentrations in $SW_{\text{unf}} + SI_{\text{unf}}$ were the same as that estimated from $(SW_{\text{f}} + SI_{\text{unf}}) + (SW_{\text{unf}} + SI_{\text{f}})$ for A (Fig. 5), suggesting no competition between the ice-derived and planktonic algal communities in A. However, *Chla* concentrations measured in $SW_{\text{unf}} + SI_{\text{unf}}$ were lower than that estimated from $(SW_{\text{f}} + SI_{\text{unf}}) + (SW_{\text{unf}} + SI_{\text{f}})$ for B (Fig. 5), indicating some competition between the ice-derived and planktonic algal communities in B. Total bacterial biomasses measured in $SW_{\text{unf}} + SI_{\text{unf}}$ were lower than that estimated from $(SW_{\text{f}} + SI_{\text{unf}}) + (SW_{\text{unf}} + SI_{\text{f}})$ (Fig. 5), especially for A, indicating a competition between the ice-derived and planktonic bacterial communities occurred, or that the grazing pressure was higher in $SW_{\text{unf}} + SI_{\text{unf}}$. The biomass of heterotrophic nanoflagellates, grazers of bacteria, actually increased 11-fold in $SW_{\text{unf}} + SI_{\text{unf}}\text{-A}$ after 9 days, therefore supporting the latter hypothesis.

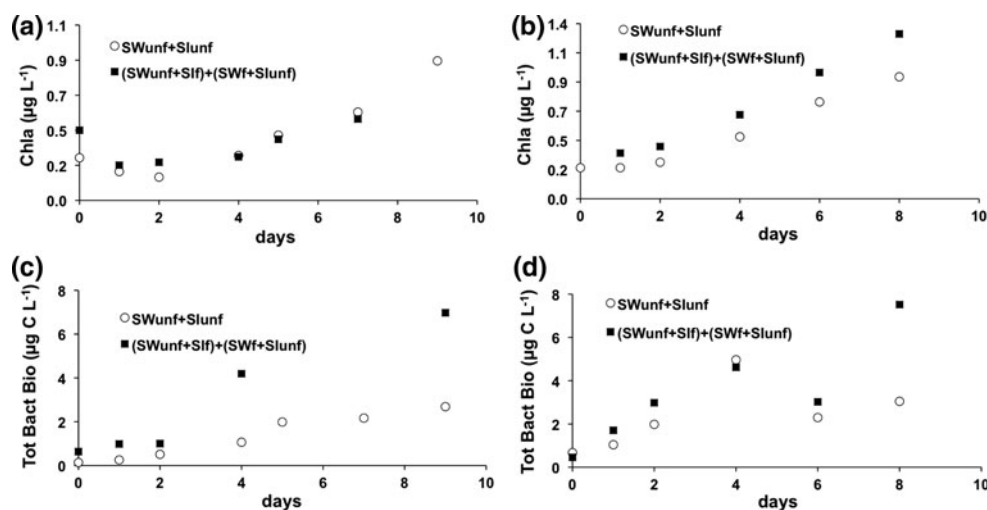
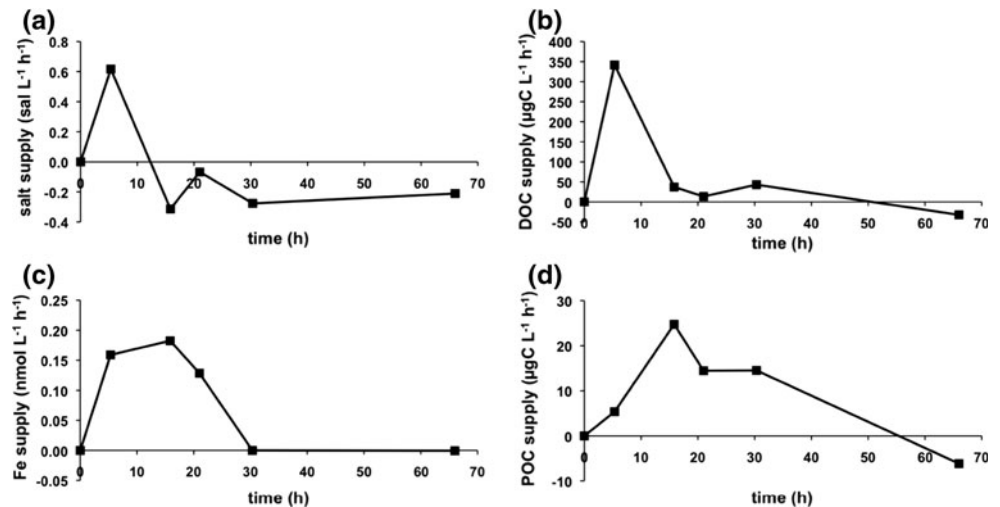


Fig. 5 **a** Chlorophyll *a* in the microcosms $SW_{\text{unf}} + SI_{\text{unf}}$ and $(SW_{\text{f}} + SI_{\text{unf}}) + (SW_{\text{unf}} + SI_{\text{f}})$ in experiment A, **b** Chlorophyll *a* in the microcosms $SW_{\text{unf}} + SI_{\text{unf}}$ and $(SW_{\text{f}} + SI_{\text{unf}}) + (SW_{\text{unf}} + SI_{\text{f}})$ for experiment B, **c** total bacterial biomass in the microcosms $SW_{\text{unf}} + SI_{\text{unf}}$ and $(SW_{\text{f}} + SI_{\text{unf}}) + (SW_{\text{unf}} + SI_{\text{f}})$ for experiment A

and **d** total bacterial biomass in the microcosms $SW_{\text{unf}} + SI_{\text{unf}}$ and $(SW_{\text{f}} + SI_{\text{unf}}) + (SW_{\text{unf}} + SI_{\text{f}})$ for experiment B. This figure aims at estimating the level of competition between ice-derived and planktonic microorganisms

Fig. 6 Fluxes of **a** salts, **b** dissolved organic carbon (DOC), **c** total dissolvable iron (Fe) and **d** particulate organic carbon (POC) during the melting experiment. We observe a decoupling between the release of DOC and POC



Sequential melting

In order to magnify the release of the sea ice constituents, we melted a 20-cm-thick section of brown ice (14 cm diameter) in 13.5 L of seawater (sea ice to seawater volume ratio $\approx 1:10$ corresponds to about 1 m thick ice cover melting in 10 m deep seawater). Depending on the sea ice thickness and the depth of the mixed layer, this ratio may vary widely in the field. In situ DOC, POC and TDFe concentrations may also vary in space and time. It is therefore important to note that while the fluxes presented here are adequately used to compare the timing of release of the sea ice constituents, the actual numbers are not representative of the in situ fluxes.

Figure 6 shows a supply in salts after 5 h, due to gravity-driven brine drainage (brine salinity > seawater salinity). This was followed by a supply of fresher water due to the melting of the ice matrix itself, less saline than seawater. We observe a decoupling between the release of dissolved and particulate organic matter. Maximal flux was reached after 5 h for DOC, but after 15 h for POC. After 20 h, the fluxes of organic matter decreased strongly. DOC flux even became negative, indicating a quicker degradation of DOC in the reactor than in the control bottle. TDFe supply was maximal between 5 and 15 h ($0.18 \text{ nmol L}^{-1} \text{ h}^{-1}$). Nil Fe flux is reached after 30 h of melting.

Discussion

In situ distribution of microbial communities

A decrease of Fe and organic carbon concentrations in sea ice was observed (Table 2). Sea ice biomass did not seem to increase between the 29 November and 30 December despite improving conditions of temperature, light and brine volume fraction (Table 2). Krembs et al. (2001) and

Becquevort et al. (2009) pointed that algal development in sea ice might be controlled by space availability: i.e. algal growth is favoured when brine volume fractions >8 %, roughly corresponding to ice temperature $>-4 \text{ }^\circ\text{C}$. Because the brine volume fraction is relatively high throughout this survey, the stagnation of the algal stock may be due to nutrient limitation. Loss of organic matter during ice melting and/or grazing pressure can also play a role as suggested by the high biomass of heterotrophic dinoflagellates measured in bottom ice on 30 December.

The distribution of algal species varied along the cores collected during ISPOL; however, seasonal variability was low during our time series (Fig. 2). Although their relative dominance varied, some algal species present in sea ice were also found in seawater, indicating a seeding from sea ice. For example, the in situ 30 m deep seawater showed an increase with time of the pennate diatoms biomass, which is the main algal group observed in bottom sea ice (Fig. 2). *Phaeocystis* sp. and flagellates seem to also develop in seawater. Such parallel between sea ice and seawater algal communities has already been observed in numerous studies and formed the basis of the seeding hypothesis (Garrison and Buck 1985; Smith and Nelson 1986; Garrison et al. 1987).

Fate of ice constituents during and after sea ice melting

Autotrophs

The Chl*a* increase in the microcosm $\text{SW}_f + \text{SI}_{\text{unf}}$ confirms that at least a fraction of the sea ice community can grow in seawater (Fig. 4). This confirms results reported in Kuosa et al. (1992), although the increase in algal biomass in our trace-metal clean study was less important than in Kuosa's study. The increase of autotrophic biomass in $\text{SW}_f + \text{SI}_{\text{unf}}$ was mainly attributable to species $<10 \text{ } \mu\text{m}$ (Fig. 4). The

decrease of $>10\ \mu\text{m}$ algae can be due to the lower Fe concentrations experienced in seawater compared to sea ice (large cells have a higher Fe demand than small ones; Sunda and Huntsman 1995). Iron concentrations in our microcosms were relatively high, but can be limiting for large ice algae, which are accustomed to Fe concentrations up to 2 orders of magnitude higher than in seawater. In the sea ice environment, sedimentation processes may be particularly efficient because of the production of exopolysaccharides (EPS) by sea ice algae (Palmisano and Sullivan 1985a; Krembs et al. 2001). EPS can stimulate the formation of aggregates (Passow 2002) and export as observed in rolling tanks (Riebesell et al. 1991) and silicon isotope measurements (Fripiat et al. 2007). Our field data also showed that sea ice diatoms were not systematically prevailing in surface seawater, most likely because they were rapidly exported below the mixed layer or were grazed immediately (Fig. 1). In the natural environment, the intensity of grazing by copepods, amphipods or krill can greatly influence the recycling of organic material and Fe in surface waters (Lizotte 2003; Thomas and Papatimitriou 2003; Tovar-Sanchez et al. 2007; Lannuzel et al. 2010). Heavily grazed blooms can retain more biogenic elements in the surface layer, whereas ungrazed diatoms tend to sink out (Smetacek and Nicol 2005). Faecal pellets from these organisms can, however, contribute to the export of C to the depths.

Heterotrophs

Table 3 shows that at the start of the experiments, pack ice supplied much less heterotrophs than autotrophs, with even lower bacterial biomass when sea ice was added to the microcosm (Table 3). Figure 4 shows an increase in the ice-derived bacterial biomass with time, while the bacterial cell volume decreased in the microcosm $\text{SW}_f + \text{SI}_{\text{unf}}$. This decrease in cell volumes can be attributed to a decrease in the concentration of labile substrates such as the DOC (Roszak and Colwell 1987; Berman et al. 1994) or size-selective grazing by protozoa (Gonzales et al. 1990). This latter scenario is supported by the higher protozoa biomass where the highest decrease in the bacterial biovolume is observed at the end of the experiment. Grazing by protozoa is also most probably responsible for the lower initial biomasses of phytoplankton and bacteria in the microcosms (Table 2) than in situ (Fig. 4). The effect of seeding on bacteria is poorly documented. Phylogenetic studies showed that sea ice bacterial population is similar to the seawater community (Bowman et al. 1997), metabolically active (Brinkmeyer et al. 2003) and that psychrophilic species were preferentially present in sea ice (Delille 1992; Helmke and Weyland 1995). Kaartokallio et al. (2005) reported that, in Baltic sea ice, ice-derived bacterial

communities were able to adapt to salinity changes while under-ice bacterial assemblages seemed to suffer from osmotic stress. Physiological and community structure changes in response to a changing environment (e.g. salinity) will occur during the melting of sea ice (Kaartokallio et al. 2005).

Organic matter and Fe

Similar to other Antarctic pack ice field studies (e.g. Lannuzel et al. 2007; Becquevort et al. 2009; van de Merwe et al. 2011a, b), large accumulation in sea ice of both organic matter and Fe was reported during the ISPOL survey (Table 2; Arrigo and Thomas 2004; Lannuzel et al. 2008; Dumont et al. 2009), indicating that sea ice can be a significant source of organic matter and Fe to the phytoplankton-poor and Fe-starved Antarctic surface waters. Dissolved organic matter can originate from melting sea ice but also from excretion by phytoplankton, sea ice algal cell lysis, exudation or sloppy feeding by zooplankton (Kähler et al. 1997). The release of Fe from melting sea ice has been addressed by several authors (e.g. Sedwick and DiTullio 1997) and quantified in many studies (Lannuzel et al. 2007; 2008; 2010; van der Merwe et al. 2011a, b). In the Fe-limited Antarctic waters, this seasonal pulse of nutrients can trigger phytoplankton blooms, as confirmed during the ISPOL time series, our microcosms experiments and spring/summer satellite imagery of the marginal ice zone. Figure 4 shows that autotrophic and bacterial biomasses are stimulated in the microcosm amended with filtered sea ice. Algal growth can be triggered by (1) the supply of micronutrients such as Fe, (2) less grazing pressure (Giesenhagen et al. 1999) and (3) the stimulation of heterotrophic processes through the release of labile sea ice-derived DOM (Brandini and Baumann 1997), which will supply essential molecules for the autotrophs (e.g. siderophores or cytokines). In HNLC waters, carbon seemed to be the first limiting factor for bacterial growth, although Fe can quickly become limiting when carbon limitation is alleviated (Church et al. 2000; Kirchman et al. 2000; Becquevort et al. 2007). We note that the effect of melting sea ice is also observed between microcosms A and B, with higher bacterial and algal biomasses in B (Table 3). Field data confirmed that sea ice melting was well underway when arriving on site on the 29 November, releasing 70 % of Fe in surface seawater within the first 10 days of the time series (Lannuzel et al. 2008). Our microcosms samples were collected after this initial Fe fertilization. Therefore, the 1 % sea ice inoculation would have only contributed to an increase of 4–5 % of the initial seawater concentration of Fe in the microcosms A and B. Note that the Fe concentrations in seawater were already relatively high (i.e. non-limiting for phytoplankton growth)

compared to ice-free waters (typically $0.1\text{--}0.2\text{ nmol L}^{-1}$), particularly at the start of experiment B (Table 2). We come to the conclusion that the direct supply of Fe from sea ice represents an addition of only 4–5 % of the initial concentrations of Fe in the microcosms. The contribution of ice-derived Fe is therefore not significant this late in the melting season. Instead, we believe that ice-derived DOM stimulated the bacterial and algal growths observed in the microcosm $\text{SW}_{\text{unf}} + \text{SI}_f$.

Sequential melting

In our microcosm experiments, all the sea ice constituents (microorganisms, DOM and Fe) were released simultaneously into the water column. Sea ice melting is, however, not an instantaneous but rather a sequential process; the release of the sea ice constituents relies on the brine movement within the ice and at the ice-water interface (i.e. drainage, convection and diffusion processes). The main question is in which order organic and inorganic elements embedded in the gel-matrix in sea ice are released in seawater. Iron could well be released with the dense brines and rapidly exported towards deeper waters, and therefore not available for phytoplankton uptake. If Fe is released before sea ice microorganisms, then this nutrient supply is not beneficial for the sea ice community anymore. But if the release of Fe is slow, then it could be maintained in the surface water owing to the enhanced stratification and therefore be used by water-based and sea ice-based microorganisms. Riebesell et al. (1991) observed the release of the ice algae before the complete melting of the ice sheet, hence before the stabilization of the mixed layer. The same was observed in the case of Fe during the ISPOL time series, where 70 % of Fe was released while the sea ice cover was still present (Lannuzel et al. 2008).

In the laboratory-based sequential melting experiment, we observed a decoupling between DOC and POC. Brine drainage is the first process at work to release salts as well as DOC (5 h), while POC was released at a later stage (15 h). As TDFe includes both the truly dissolved and particulate leachable fractions, dissolved Fe was released first together with DOC (maximum at 5 h), while particulate leachable Fe was released with POC at a later stage (maximum at 15 h). This decoupling between the dissolved and particulate Fe phase has been reported in the field (van der Merwe et al. 2011a). We note that some low-salinity water was released at the same time as the maximal fluxes of POC and particulate Fe (at 15 h), possibly inducing a stabilization of the mixed layer before complete melting of sea ice is achieved (Fig. 6). This result also confirms field observations. We conclude that the 2-stage release of Fe favours both the sea ice- and seawater-based communities.

Several factors can increase the efficiency of the fertilization of the Antarctic surface waters: (1) the thinning of the mixed layer when freshwater is added also reduces the cellular Fe demand of pelagic algae required in light harvesting processes (Raven 1990); (2) Fe is released into seawater together with organic ligands, which increase the residence time of Fe in surface waters and therefore its bio-availability (van der Merwe et al. 2009; Hassler et al. 2011). The production of exopolysaccharides (EPS) by sea ice algae, however, stimulates the formation of aggregates and therefore lead to rapid sedimentation of ice-derived Fe (Riebesell et al. 1991; Meiners et al. 2004); and (3) heterotrophic activity in seawater favours the remineralization of Fe associated with ice-derived organic matter.

Conclusion

This paper presents the first results on microcosms experiments performed under trace-metal clean conditions. Our main findings are as follows: (1) pack ice supplies much less heterotrophs than autotrophs, (2) small ice algae ($<10\text{ }\mu\text{m}$) and ice bacteria can grow in seawater, (3) planktonic algal and bacterial growths are stimulated by ice-derived DOM, (4) the contribution of Fe from melting sea ice is not significant in our microcosms experiments because most of the Fe was already released before our arrival on site and (5) dissolved and particulate sea ice constituents are released sequentially favouring both the sea ice- and seawater-based communities. Future studies should include the impact of grazing by zooplankton and sedimentation processes on the Fe and carbon cycling in the marginal ice zone. Additional work should also focus on the bio-availability of Fe in the sea ice environment, with special emphasis on size partitioning (soluble, dissolved and particulate), organic speciation and redox state (Fe^{2+} and Fe^{3+}) of Fe.

Acknowledgments The authors are grateful to the officers and crews of the RV *Polarstern* for their logistic assistance during the ISPOL cruise. We would like to thank the Alfred Wegener Institute, especially Michael Spindler, David Thomas and Gerhard Dieckmann for allowing us to take part in the ISPOL cruise. This work was carried out in the framework of the Belgian research programme Action de Recherche Concertée “Sea Ice Biogeochemistry in a CLIMate change perspective” financed by the Belgian French Community under contract n°ARC-02/7-318287. This is also a contribution to the European Network of Excellence EUR-OCEANS (contract n°511106-2) and to the BELCANTO (contracts SD/CA/03A&B) and BIGSOUTH (contract N° SD/CA/05A) projects financed by the Belgian Federal Science Policy Office. The present study is a Belgian input to the Surface Ocean Low Atmosphere Study international research initiative. Isabelle Dumont was supported by a Fonds pour la Recherche en Industries Agronomiques grant. Bruno Delille is a F.R.S-FNRS Research Associate.

Open Access This article is distributed under the terms of the Creative Commons Attribution License which permits any use, distribution, and reproduction in any medium, provided the original author(s) and the source are credited.

References

- Arrigo KR, Thomas DN (2004) Large scale importance of biology in the Southern Ocean. *Antarct Sci* 16(4):471–486
- Arrigo KR, Mock T, Lizotte MP (2010) Primary producers and sea ice. In: Thomas DN, Dieckmann GS (eds) *Sea ice*. Blackwell Sci, Oxford, UK, pp 283–326
- Becquevort S, Lancelot C, Schoemann V (2007) The role of iron in the bacterial degradation of organic matter derived from *Phaeocystis antarctica*. *Biogeochemistry* 83:119–135
- Becquevort S, Dumont I, Tison J-L, Lannuzel D, Sauvée M-L, Chou L, Schoemann V (2009) Biogeochemistry and microbial community composition in sea ice and underlying seawater off East Antarctica during early spring. *Polar Biol* 32:879–895
- Berman T, Hoppe HG, Gocke K (1994) Response of aquatic bacterial-populations to substrate enrichment. *Mar Ecol Prog Ser* 104:173–184
- Bowman JP, McCammon SA, Brown MV, Nichols DS, McMeekin TA (1997) Diversity and association of psychrophilic-bacteria in Antarctic sea ice. *Appl Environ Microbiol* 63:3068–3078
- Brandini FP, Baumann MEM (1997) The potential role of melted “brown ice” as sources of chelators and ammonia to the surface waters of the Weddell Sea, Antarctica (18th Symposium on Polar Biology). *Proceedings of the NIPR symposium on polar biology* 10:1–13
- Brinkmeyer R, Knittel K, Jurgens J, Weyland H, Amann R, Helmke E (2003) Diversity and structure of bacterial communities in arctic versus antarctic pack ice. *Appl Environ Microbiol* 69:6610–6619
- Church MJ, Hutchins DA, Ducklow HW (2000) Limitation of bacterial growth by dissolved organic matter and iron in the Southern Ocean. *Appl Environ Microbiol* 66:455–466
- Cox GFN, Weeks WF (1988) Numerical simulations of the profile properties of undeformed first-year sea ice during the growth season. *J Geophys Res* 93(C10):12449–12460
- de Jong J, Schoemann V, Tison J-L, Lannuzel D, Mattioli N (2008) High-accuracy determination of iron in seawater by isotope dilution multiple collector inductively coupled plasma mass spectrometry (ID-MC-ICP-MS) using nitrilotriacetic acid chelating resin for pre-concentration and matrix separation. *Anal Chim Acta* 623:126–139
- Delille D (1992) Marine bacterioplankton at the Weddell Sea ice edge, distribution of psychrophilic and psychrotrophic populations. *Polar Biol* 12:205–210
- Dumont I, Schoemann V, Lannuzel D, Chou L, Tison JL, Becquevort S (2009) Distribution and characterization of dissolved and particulate organic matter in Antarctic pack ice. *Polar Biol* 32(5):733–750
- Eicken H (2003) From the microscopic, to the macroscopic, to the regional scale: growth, microstructure, and properties of sea ice. In: Thomas DN, Dieckmann GS (eds) *Sea ice—an introduction to its physics, chemistry, biology and geology*. Blackwell Science, Oxford, pp 22–83
- Fripiat F, Cardinal D, Tison JL, Worby A, Andre L (2007) Diatom-induced silicon isotopic fractionation in Antarctic sea ice. *J Geophys Res-Biogeosci* 112:G02001
- Garrison DL, Buck KR (1985) Sea-ice algal communities in the Weddell Sea: species composition in ice and plankton assemblages. In: Gray JS, Christiansen ME (eds) *Marine biology of polar regions and effects of stress on marine organisms*. J Wiley, New York, pp 103–122
- Garrison D, Buck KR, Fryxell GA (1987) Algal assemblages in Antarctic pack ice and in-edge plankton. *J Phycol* 23:564–572
- Giesenhan HC, Detmer AE, de Wall J, Weber A, Gradinger RR, Jochem FJ (1999) How are Antarctic planktonic microbial food webs and algal blooms affected by melting of sea ice? *Microcosm simulations*. *Aquat Microb Ecol* 20:183–201
- Golden KM, Ackley SF, Lytle VI (1998) The percolation phase transition in sea ice. *Science* 282:2238–2241
- Gonzalez JM, Iriberrri J, Egea L, Barcina I (1990) Differential rates of digestion of bacteria by fresh-water and marine phagotrophic protozoa. *Appl Environ Microbiol* 56:1851–1857
- Gradinger R, Ikävalko J (1998) Organism incorporation into newly forming Arctic sea ice in the Greenland Sea. *J Plankton Res* 20:871–886
- Hassler CS, Schoemann V, Mancuso-Nichols C, Butler ECV, Boyd PW (2011) Saccharides enhance iron bioavailability to Southern Ocean phytoplankton. *Proc Natl Acad Sci* 108:1076–1081
- Hellmer HH, Schroder M, Haas C, Dieckmann GS, Spindler M (2008) The ISPOL drift experiment. *Deep-Sea Res II*(55):913–917
- Helmke E, Weyland H (1995) Bacteria in sea-ice and underlying water of the eastern Weddell Sea in midwinter. *Mar Ecol Prog Ser* 117:269–287
- Hillebrand H, Dürselen C-D, Kirschtel D, Pollinger U, Zohary T (1999) Biovolume calculation for pelagic and benthic microalgae. *J Phycol* 35:403–424
- Kaartokallio H, Laamanen M, Sivonen K (2005) Responses of Baltic Sea ice and open-water natural bacterial communities to salinity change. *Appl Environ Microbiol* 71:4364–4371
- Kahler P, Bjornsen PK, Lochte K, Antia A (1997) Dissolved organic matter and its utilization by bacteria during spring in the Southern Ocean. *Deep-Sea Res II* 44:341–353
- Kirchman DL, Meon B, Cottrell MT, Hutchins DA, Weeks D, Bruland KW (2000) Carbon versus iron limitation of bacterial growth in the California upwelling regime. *Limnol Oceanogr* 45:1681–1688
- Krembs C, Mock T, Gradinger R (2001) A mesocosm study of physical–biological interactions in artificial sea ice: effects of brine channel surface evolution and brine movement on algal biomass. *Polar Biol* 24:356–364
- Kuosa H, Norrman B, Kivi K, Brandini F (1992) Effects of Antarctic sea ice biota on seeding as studied in aquarium experiments. *Polar Biol* 12:333–339
- Lancelot C, Mathot S, Veth C, de Baar H (1993) Factors controlling phytoplankton ice-edge blooms in the marginal ice-zone of the Northwestern Weddell Sea during sea-ice retreat 1988—field observations and mathematical-modeling. *Polar Biol* 13:377–387
- Lancelot C, de Montety A, Goosse H, Becquevort S, Schoemann V, Pasquer B, Vancoppenolle M (2009) Spatial distribution of the iron supply to phytoplankton in the Southern Ocean: a model study. *Biogeosci Discuss* 6:4919–4962
- Lannuzel D, de Jong J, Schoemann V, Trevena A, Tison JL, Chou L (2006) Development of a sampling and flow injection analysis technique for iron determination in the sea ice environment. *Anal Chim Acta* 556:476–483
- Lannuzel D, Schoemann V, de Jong J, Tison JL, Chou L (2007) Distribution and biogeochemical behaviour of iron in the East Antarctic sea ice. *Mar Chem* 106:18–32
- Lannuzel D, Schoemann V, de Jong J, Chou L, Delille B, Becquevort S, Tison JL (2008) Iron study during a time series in the western Weddell pack ice. *Mar Chem* 108:85–95
- Lannuzel D, Schoemann V, Pasquer B, van der Merwe P, Bowie AR (2010) What controls the distribution of dissolved iron in the seasonal ice zone? Spatial, seasonal and inter-annual variability. *J Geophys Res* 115:G03022. doi:10.1029/2009JG001031
- Lizotte MP (2003) The microbiology of sea ice. In: Thomas DN, Dieckmann GS (eds) *Sea ice—an introduction to its physics,*

- chemistry, biology and geology. Blackwell Science Ltd, Oxford, pp 184–210
- Martin JH, Fitzwater SE, Gordon RM (1990) Iron deficiency limits phytoplankton growth in Antarctic waters. *Global Biogeochem Cycles* 4(1): 5–12, 10
- Mathot S, Becquevort S, Lancelot C (1991) Microbial communities from the sea ice and adjacent water column at the time of ice melting in the northwestern part of the Weddell Sea. *Polar Res* 10:267–275
- Meiners K, Brinkmeyer R, Granskog MA, Lindfors A (2004) Abundance, size distribution and bacterial colonization of exopolymer particles in Antarctic sea ice (Bellingshausen Sea). *Aquat Microb Ecol* 35(3):283–296
- Menden-Deuer S, Lessard EJ (2000) Carbon to volume relationships for dinoflagellates, diatoms, and other protist plankton. *Limnol Oceanogr* 45:569–579
- Palmisano AC, Sullivan CW (1985) Pathways of photosynthetic carbon assimilation in sea-ice microalgae from McMurdo Sound, Antarctica. *Limnol Oceanogr* 30:674–678
- Passow U (2002) Transparent exopolymer particles (TEP) in aquatic environments. *Prog Oceanogr* 55:287–333
- Porter KG, Feig YS (1980) The use of DAPI for identifying and counting aquatic microflora. *Limnol Oceanogr* 25:943–948
- Raven JA (1990) Predictions of Mn and Fe use efficiencies of phototrophic growth as a function of light availability for growth and of C assimilation pathway. *New Phytol* 116:1–18
- Riebesell U, Schloss I, Smetacek V (1991) Aggregation of algae released from melting sea ice—implications for seeding and sedimentation. *Polar Biol* 11:239–248
- Roszak DB, Colwell RR (1987) Survival strategies of bacteria in the natural environment. *Microbiol Rev* 51:365–379
- Róžańska M, Poulin M, Gosselin M (2008) Protist entrapment in newly formed sea ice in the Coastal Arctic Ocean. *J Mar Syst* 74:887–901
- Schlitzer R (2008) Ocean data view, <http://odv.awi.de>
- Sedwick PN, DiTullio GR (1997) Regulation of algal blooms in Antarctic shelf waters by the release of iron from melting sea ice. *Geophys Res Lett* 24:2515–2518
- Simon M, Azam F (1989) Protein-content and protein-synthesis rates of planktonic marine-bacteria. *Mar Ecol Prog Ser* 51:201–213
- Smetacek V, Nicol S (2005) Polar ocean ecosystems in a changing world. *Nature* 437:362–368
- Smith WO, Nelson DM (1986) Importance of ice edge phytoplankton blooms in the Southern Ocean. *Bioscience* 36:251–257
- Sugimura Y, Suzuki Y (1988) A high-temperature catalytic-oxidation method for the determination of non-volatile dissolved organic-carbon in seawater by direct injection of a liquid sample. *Mar Chem* 24:105–131
- Sunda WG, Huntsman SA (1995) Iron uptake and growth limitation in oceanic and coastal phytoplankton in seawater. *Mar Chem* 50:189–206
- Thomas DN, Papadimitriou S (2003) Biogeochemistry of sea ice. In: Thomas DN, Dieckmann GS (eds) *Sea ice—an introduction to its physics, chemistry, biology and geology*. Blackwell Science Ltd, Oxford, pp 267–302
- Tison JL, Worby A, Delille B, Brabant F, Papadimitriou S, Thomas D, de Jong J, Lannuzel D, Haas C (2008) Temporal evolution of decaying summer first-year sea ice in the Western Weddell Sea, Antarctica. *Deep Sea Res II* 55:975–987
- Tovar-Sánchez A, Duarte CM, Hernández-León S, Sañudo-Wilhelmy SA (2007) Krill as a central node for iron cycling in the Southern Ocean. *Geophys Res Lett* 34:L11601
- Utermöhl H (1958) Zur Vervelkommnung der quantitativen Phytoplankton-Methodik. *Mitt Int Verein Theor Angew Limnol* 9:1–38
- van der Merwe P, Lannuzel D, Mancuso Nichols CA, Meiners K, Heil P, Norman L, Thomas D, Bowie AR (2009) Biogeochemical observations during the winter-spring transition in East Antarctic sea ice: implications of exopolysaccharides. *Mar Chem* 15(3-4):163–175
- van der Merwe P, Lannuzel D, Mancuso Nichols CA, Meiners K, Bowie AR (2011a) Iron fractionation in pack and fast ice in East Antarctica: potential for temporal decoupling between the release of dissolved and particulate iron during spring melt. *Deep Sea Res II* 58(9–10):1222–1236
- van der Merwe P, Lannuzel D, Bowie AR, Meiners KM (2011b) High temporal resolution observations of spring fast ice melt and seawater iron enrichment in East Antarctica. *J Geophys Res* 116:G03017. doi:10.1029/2010JG001628
- Watson SW, Novitsky TJ, Quinby HL, Valois FW (1977) Determination of bacterial number and biomass in the marine environment. *Appl Environ Microbiol* 33:940–946
- Yentsch CS, Menzel DW (1963) A method for the determination of phytoplankton chlorophyll and phaeophytin by fluorescence. *Deep Sea Res Oceanogr Abstr* 10(3):221–231